

Metabolic Modeling Identifies Key Constraints on an Engineered Glycine Betaine Synthesis Pathway in Tobacco¹

Scott D. McNeil, David Rhodes, Brenda L. Russell², Michael L. Nuccio, Yair Shachar-Hill, and Andrew D. Hanson*

Horticultural Sciences Department, University of Florida, Gainesville, Florida 32611 (S.D.M., B.L.R., M.L.N., A.D.H.); Center for Plant Environmental Stress Physiology, Department of Horticulture and Landscape Architecture, Purdue University, West Lafayette, Indiana 47907 (D.R.); and Department of Chemistry and Biochemistry, New Mexico State University, Las Cruces, New Mexico 88003 (Y.S.-H.)

Previous work has shown that tobacco (*Nicotiana tabacum*) plants engineered to express spinach choline monooxygenase in the chloroplast accumulate very little glycine betaine (GlyBet) unless supplied with choline (Cho). We therefore used metabolic modeling in conjunction with [¹⁴C]Cho labeling experiments and in vivo ³¹P NMR analyses to define the constraints on GlyBet synthesis, and hence the processes likely to require further engineering. The [¹⁴C]Cho doses used were large enough to markedly perturb Cho and phosphocholine pool sizes, which enabled development and testing of models with rates dynamically responsive to pool sizes, permitting estimation of the kinetic properties of Cho metabolism enzymes and transport systems in vivo. This revealed that import of Cho into the chloroplast is a major constraint on GlyBet synthesis, the import rate being approximately 100-fold lower than the rates of Cho phosphorylation and transport into the vacuole, with which import competes. Simulation studies suggested that, were the chloroplast transport limitation corrected, additional engineering interventions would still be needed to achieve levels of GlyBet as high as those in plants that accumulate GlyBet naturally. This study reveals the rigidity of the Cho metabolism network and illustrates how computer modeling can help guide rational metabolic engineering design.

Daniel Koshland's recent commentary on "the era of pathway quantification" encapsulates the growing importance to basic biochemistry of mathematical tools for quantifying metabolic fluxes in vivo (1998). Moreover, advances in metabolic control theory and metabolic engineering experience show that we must quantify fluxes if we wish to understand metabolism well enough to manipulate it effectively (Fell, 1997; Nuccio et al., 1999; Stephanopoulos, 1999). No matter the approach used to investigate fluxes (e.g. radio or stable isotopes), it is generally necessary to use computer-assisted modeling to derive in vivo flux values from experimental data because there are too many variables to handle by intuition (Bailey, 1998). Here we apply computer modeling to interpret experimental radiolabeling data in a metabolic engi-

neering situation: Glycine betaine (GlyBet) synthesis in transgenic tobacco (*Nicotiana tabacum* L. cv Wisconsin 38) expressing choline (Cho) monooxygenase (CMO).

GlyBet is an established target for metabolic engineering of stress tolerance because it is a potent osmoprotectant that many plants lack (McNeil et al., 1999). In spinach, GlyBet is synthesized in the chloroplast by a two-step oxidation of Cho and catalyzed by CMO and betaine aldehyde dehydrogenase (BADH). The absence of CMO is the most obvious constraint on GlyBet production in GlyBet-deficient plants such as tobacco, but tobacco transgenics expressing CMO in chloroplasts at up to 10% of the level in spinach accumulated at most 70 nmol GlyBet g⁻¹ fresh weight, or approximately 0.3% of that in spinach (Nuccio et al., 1998). However, GlyBet levels increased greatly when Cho or its precursors mono- and dimethylethanolamine were supplied, suggesting that the endogenous Cho supply is inadequate (Nuccio et al., 1998). Similar results were obtained with tobacco and other dicots expressing a bacterial Cho oxidase in the cytosol (Huang et al., 2000).

Radiotracer and modeling studies have shown that tobacco leaves synthesize Cho moieties via parallel phosphobase (P-base) and phosphatidylbase (Ptd-base) pathways, and that the former accounts for some 85% of the total flux (McNeil et al., 2000). These pathways respectively produce phosphocholine (P-Cho) and phosphatidylcholine (Ptd-Cho; Fig.

¹ This work was supported in part by the U.S. Department of Agriculture National Research Initiative-Competitive Grants Program (grant no. 98-35100-6149 to A.D.H.), by the National Science Foundation (grant no. IBN-9813999 to A.D.H.), by the Department of Energy (grant no. DE-FG02-99ER20344 to D.R.), by a grant from the National Institute of Science and Technology (to Y.S.-H.), by an endowment from the C.V. Griffin, Sr., Foundation, and by the Florida Agricultural Experiment Station. This is journal series paper no. R-07426.

² Present address: Corning Community College, Corning, NY 14830.

* Corresponding author; e-mail adha@gnv.ifas.ufl.edu; fax 352-392-6479.

1). Free Cho, the substrate required by CMO, originates almost solely from Ptd-Cho turnover. Once released from Ptd-Cho into the cytosol, Cho is either rapidly converted to P-Cho by Cho kinase and re-used in Ptd-Cho synthesis or transported into a storage pool, presumably in the vacuole (McNeil et al., 2000). In tobacco engineered with CMO in the chloroplast the CMO must therefore compete for free Cho with both Cho kinase and vacuolar Cho transport (Fig. 1). However, since CMO is inside the chloroplast and Cho is generated in the cytosol, unless Cho crosses the chloroplast envelope freely it would be the chloroplast Cho uptake process, not CMO itself, that would be pitted against Cho kinase and vacuolar import (Fig. 1). Thus the supply of endogenous Cho for GlyBet synthesis could be limited by the rates of processes besides Cho synthesis; these include Cho phosphorylation, Cho storage in the vacuole, and Cho transport into the chloroplast.

To identify which of these processes most limit flux to GlyBet in transgenic tobacco, [^{14}C]Cho was supplied to transgenic leaf tissue, the radiolabeling kinetics of Cho, GlyBet, P-Cho, and Ptd-Cho were followed, and the data were subjected to computer modeling. This enabled us to derive a quantitative picture of the fluxes and pool sizes in the Cho metabolism network and to hypothesize how flux to GlyBet would respond to hypothetical engineered changes. A key deduction from the modeling—that the P-Cho pool is entirely cytosolic—was verified by *in vivo* ^{31}P nuclear magnetic resonance (NMR) analyses.

RESULTS AND DISCUSSION

Model Outputs and Their Implications

V_{\max} and K_m values for fluxes B through E, G, and H in the model (Table I; Fig. 2) were obtained by progressive adjustment, until the simulated radiola-

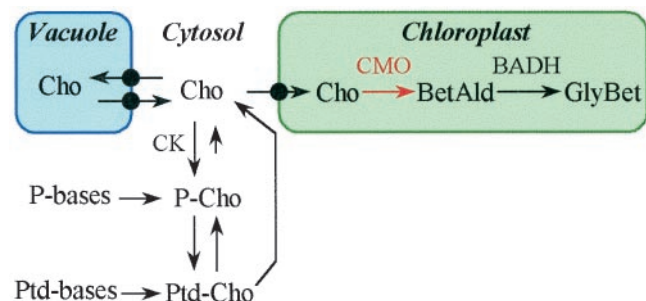


Figure 1. Cho metabolism in tobacco expressing a CMO transgene in the chloroplast. Note that the equilibrium constant for the Cho kinase (CK) reaction is approximately 10^4 (Guynn, 1976) so that P-Cho formation is strongly favored in the cytosol (Bligny et al., 1989). BetAld, Betaine aldehyde.

belonging kinetics closely matched those observed. The first order rate constants governing Cho uptake and the cytosolic Cho (Cho_{cy}) \rightarrow chloroplastic Cho (Cho_{chl}) and vacuolar Cho (Cho_{vac}) \rightarrow Cho_{cy} fluxes (fluxes A, I, and F) were obtained in the same way. Of these model-derived parameters, those for Cho kinase (flux B) and CTP:P-Cho cytidylyltransferase (flux D) can be checked against literature values. For both enzymes the modeled K_m values are close to published ones. The modeled K_m for the cytidylyltransferase of 80 nmol g^{-1} fresh weight corresponds to 3.3 mM ($80 \text{ nmol}/24 \mu\text{L} = 3.3 \text{ mM}$), which is within a factor of three of the measured K_m for P-Cho of the castor bean enzyme (1.1 mM ; Wang and Moore, 1989). The modeled K_m for Cho kinase, 1.7 mM , is within the range reported for plants ($0.03\text{--}2.5 \text{ mM}$; Setty and Krishnan, 1972; Bligny et al., 1989; Gawer et al., 1991). The modeled V_{\max} values for both enzymes also fall inside the limits known for plant tissues (e.g. Tanaka et al., 1966; Kinney et al., 1987; Bligny et al., 1989; Wang and Moore, 1989).

The success of the model in accounting for radiolabeling data is illustrated in Figure 3, which shows simulations (curves) superimposed on experimental data points for four different experiments. Figure 3, a and b show simulated and actual data for immature, unsalinized leaf tissue, for which the model was initially developed. Figure 3, c through h summarize data for salinized and mature tissue, and will be discussed later. We will turn first to the outputs of the immature leaf model.

The simulated flux rates (Fig. 4, a–e), and pool sizes (Fig. 4, f–j) during the time-course illustrate the model's usefulness in analyzing dynamic metabolic behavior. As the large dose of supplied [^{14}C]Cho is taken up (Fig. 4f), Cho_{cy} rapidly expands (Fig. 4g). This in turn drives up the rate of synthesis of P-Cho and the rates of Cho flux into the vacuole and chloroplast (Fig. 4, b–d). The transient rise in Cho_{chl} drives a matching increase in the rate of Cho oxidation to GlyBet (Fig. 4c). Elevated levels of P-Cho (Fig. 4i) increase the flux from P-Cho \rightarrow Ptd-Cho (Fig. 4d). However, since the Ptd-Cho pool is large, the expansion of the Ptd-Cho pool is modest in relative terms (Fig. 4h) and the perturbations to the Ptd-Cho \rightarrow P-Cho and Ptd-Cho \rightarrow Cho_{cy} fluxes are consequently minor (Fig. 4, d and e). When the large dose of [^{14}C]Cho has been metabolized, the fluxes and pool sizes in the model revert to a steady state (Fig. 4). The model-generated steady-state fluxes at 600 min (Fig. 4, a–e) were very similar ($r^2 = 0.98$) to the fluxes in Cho metabolism that were previously determined from ^{33}P -base and [^{14}C]formate labeling data (McNeil et al., 2000).

The following five features of the model output are significant for understanding Cho metabolism; the first four are consistent with previous analyses (McNeil et al., 2000). Taken together, all five indicate that

Table 1. Parameters used to model Cho metabolism fluxes in CMO⁺ transgenics

Fluxes are identified by the letters used in Figure 2. Units are: V_{max} values, $\text{nmol min}^{-1} \text{g}^{-1}$ fresh wt; K_m values, nmol g^{-1} fresh wt; and rate constants (fluxes A, F, and I only), min^{-1} . The V_{max} and K_m values associated with fluxes J and K (mediated by CMO and BADH, respectively) were assigned from literature data; all other values were generated by modeling.

Flux	Values							
	Immature		Immature salinized		Mature		Mature salinized	
	V_{max}	K_m	V_{max}	K_m	V_{max}	K_m	V_{max}	K_m
B	3.1	40	3.7	40	5.3	40	5.3	40
C	0.15	200	0.15	200	0.15	200	0.15	200
D	2.4	80	2	80	1.1	80	0.9	80
E	0.7	2,000	0.7	2,000	0.7	2,000	0.7	2,000
G	0.55	40	1.2	40	1	40	0.9	40
H	0.5	2,000	0.5	2,000	0.5	2,000	0.5	2,000
J	0.1	6	0.3	6	0.1	6	0.3	6
K	1	3	1	3	1	3	1	3
A ^a	0.4		0.4		0.4		0.4	
F ^a	0.0011		0.0011		0.0015		0.0011	
I ^a	0.00017		0.00038		0.00025		0.00020	

^a Tabulated values are first order rate constants.

the Cho metabolism network in tobacco is rigid as defined by Stephanopoulos and Vallino (1991); having evolved to meet demands for Ptd-Cho synthesis and turnover, it tends intrinsically to resist redirection of flux. (a) The cytosolic P-Cho pool is always substantial, and its main fate is conversion to Ptd-Cho, not Cho_{cy}. (b) The Cho_{cy} pool returns to a very low value regardless of the starting Cho_{cy} value used to prime the model at $t = 0$ min (not shown), whereas the Cho_{vac} pool reaches a near steady state of approximately 80 nmol g^{-1} fresh weight (Fig. 4g). This

confirms that the Cho_{cy} pool is normally only a small fraction of the total Cho. (c) Ptd-Cho is catabolized to P-Cho and Cho_{cy} at similar and substantial rates, resulting in a Ptd-Cho turnover rate of approximately 50% per day, which is typical for plants (e.g. Mongrand et al., 1997). (d) The net rate of Ptd-Cho synthesis is adequate to meet the Ptd-Cho requirement for growth, which is approximately 90 to $160 \text{ pmol min}^{-1} \text{g}^{-1}$ fresh weight, assuming a leaf growth rate of $10\% \text{ d}^{-1}$ (McNeil et al., 2000). (e) Flux to GlyBet is highly sensitive to changes in the rate con-

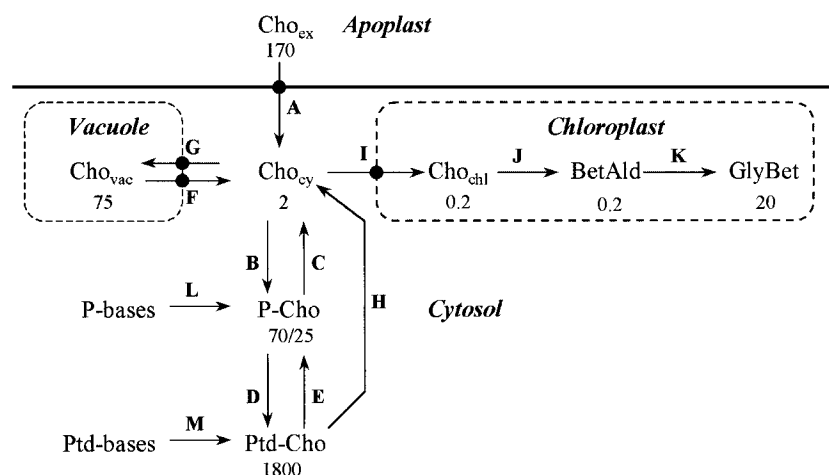


Figure 2. Schematic of the metabolic model developed for the [¹⁴C]Cho labeling experiments. Numbers beneath metabolites are initial pool sizes (nmol g^{-1} fresh weight); where two numbers are separated by a slash, the first refers to non-salinized and the second to salinized plants. The GlyBet pool size was for simplicity assumed to be 20 nmol g^{-1} fresh weight in both immature and mature leaves since this parameter makes almost no difference to the model. [¹⁴C]Cho (specific activity 54 nCi nmol^{-1}) was supplied exogenously. Note that cellular Cho is partitioned into three separate pools corresponding to cytosol (Cho_{cy}), vacuole (Cho_{vac}), and chloroplast (Cho_{chl}). Letters next to arrows denote fluxes; L and M represent the endogenous P-base and Ptd-base N-methylation pathway fluxes, which were assumed to remain constant at 0.12 and $0.02 \text{ nmol min}^{-1} \text{g}^{-1}$ fresh weight, respectively (McNeil et al., 2000). Cho uptake and the fluxes from Cho_{cy} to Cho_{chl} and Cho_{vac} to Cho_{cy} were modeled as processes with first-order dependence on the Cho substrate pool size; other fluxes were assumed to show Michaelian responses to substrate pool size.

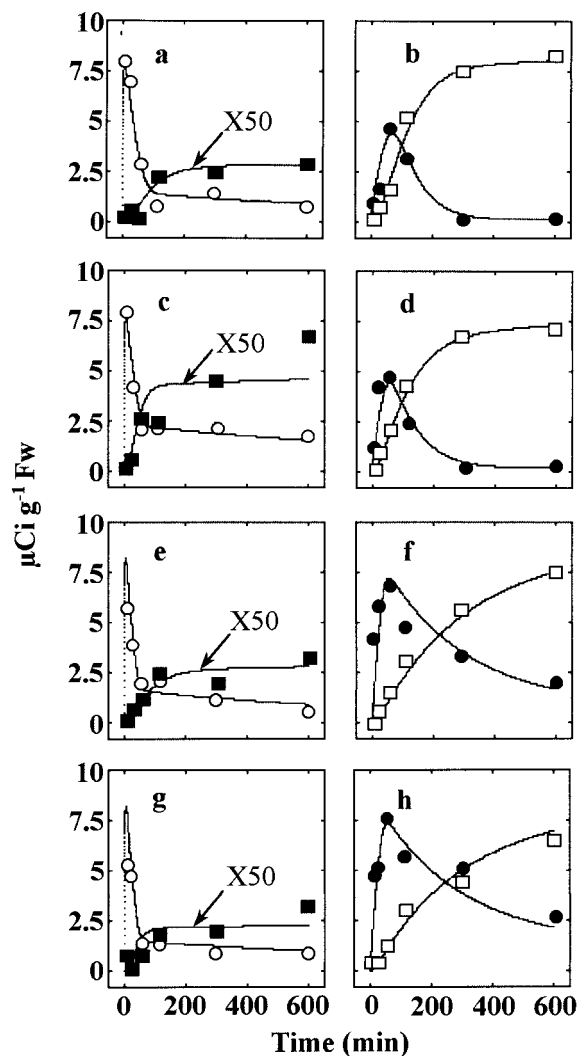


Figure 3. Simulation of the metabolism of [^{14}C]Cho in leaf discs from CMO^+ plants. Model parameters were as specified in Figure 2 and Table I. Discs were from half-expanded leaves of unsalinized (a and b) and salinized plants (c and d), or fully expanded leaves of unsalinized (e and f) and salinized (g and h) plants. Simulated time-courses (curves) are superimposed on observed radioactivities recovered in total Cho (\circ), P-Cho (\bullet), Ptd-Cho (\square), and GlyBet (\blacksquare); note that the data for GlyBet are multiplied $\times 50$.

stant describing Cho transport into the chloroplast, but not to the V_{\max} or K_m assigned to CMO and BADH. (The flux split $\text{Cho}_{\text{cy}} \rightarrow \text{P-Cho}:\text{Cho}_{\text{cy}} \rightarrow \text{Cho}_{\text{vac}}:\text{Cho}_{\text{cy}} \rightarrow \text{Cho}_{\text{chl}}$ was 84.8:15:0.2. This flux split did not change when simulations were run with 10-fold higher V_{\max} values for CMO and BADH or when Cho_{cy} was increased 10-fold.) This clearly points to the chloroplast Cho import process as the step with most control of flux through the GlyBet pathway in CMO^+ tobacco. Moreover, during steady-state conditions Cho flux across the chloroplast membrane (flux I) is approximately 380-fold less than to P-Cho (flux B) and approximately 70-fold less than to the vacuole (flux G), which indicates that the chloroplast

Cho uptake process competes poorly for Cho_{cy} with Cho kinase and vacuolar Cho transport.

Testing the Model: Application to Other Experimental Data Sets

The robustness of the model was tested by examining its ability to simulate the labeling patterns obtained in [^{14}C]Cho experiments with immature leaf tissue from salinized CMO^+ plants, salinization being known to increase CMO activity 3- to 5-fold and to reduce the P-Cho pool size 3-fold (Nuccio et al., 1998). After making these changes to the model a good fit was obtained between model-generated and observed values (Fig. 3, c and d) using parameters that were very similar to those used for unsalinized immature leaf tissue (Table I). Minor exceptions were the rate constant for Cho movement across the chloroplast envelope and the V_{\max} for Cho transport into the vacuole, both of which were about 2-fold higher in the salinized tissue. Similar tests of the model were made with data from [^{14}C]Cho experiments with unsalinized and salinized mature leaf tissue (Fig. 3, e-h). In these instances also, the observed labeling patterns were simulated satisfactorily without making major changes to the model parameters (Table I). The largest changes needed were a doubling of the V_{\max} for Cho kinase, and a halving of that for the cytidyltransferase. Lastly the model was tested by supplying larger [^{14}C]Cho doses, which increased the amount absorbed to as much as 4000 nmol g^{-1} fresh weight. Again the labeling patterns in these experiments were satisfactorily modeled (not shown).

Testing the Model: Localizing the P-Cho Pool

The model above accounts for the radiolabeling patterns seen for immature and mature leaves of unsalinized or salinized CMO^+ plants, but the model values shown are far from the only possible solutions that fit the data. It was therefore crucial to test, to the extent possible, the model's hypotheses and assumptions, and preferably to do so by means independent of radiolabeling data. A major model-generated hypothesis is that leaf tissue supplied with excess Cho will accumulate cytoplasmic P-Cho at a linear rate of at least 2.4 nmol $\text{min}^{-1} \text{g}^{-1}$ fresh weight for several hours (Fig. 4d). This prediction was directly tested by *in vivo* ^{31}P -NMR using leaf tissue strips perfused with Cho.

We made use of the pH sensitivity of certain NMR signals to distinguish vacuolar from cytoplasmic P-Cho accumulation. Figure 5A shows a ^{31}P *in vivo* NMR spectrum of tobacco leaf tissue, and Figure 5B is a series of subspectra of the phosphomonoester signals during a time-course of perfusion with Cho. The observed accumulation of a P-Cho signal over several hours is quantitatively consistent with the model's predictions (Fig. 5B, legend), and also with the elevated P-Cho

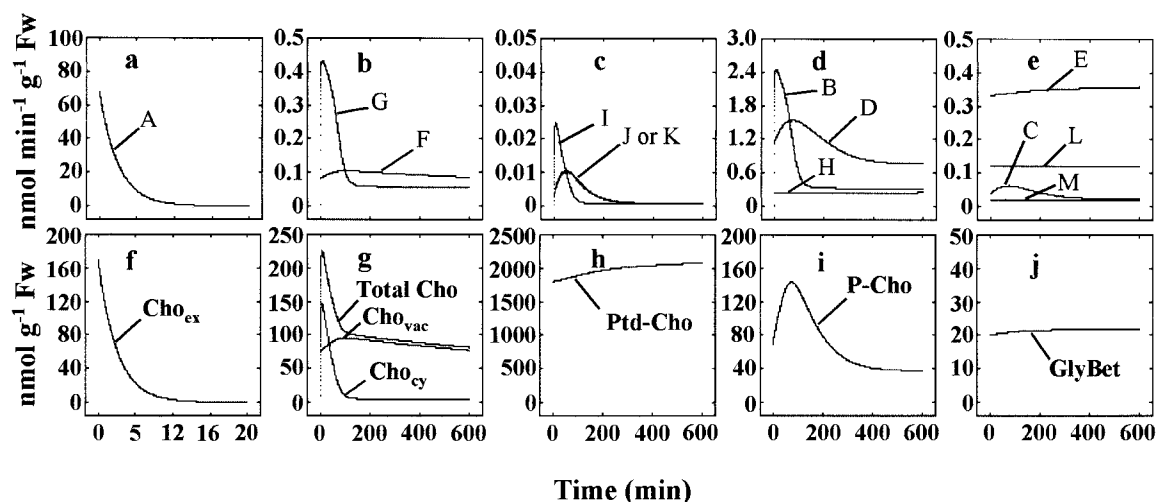


Figure 4. Simulated changes in network reaction and transport rates (a–e) and pool sizes of metabolites (f–j) during the metabolism of 170 nmol g^{-1} fresh weight of $[^{14}\text{C}]\text{Cho}$ supplied to leaf discs from one-half-expanded leaves of non-salinized CMO^+ tobacco plants. Simulated values were obtained using the model shown in Figure 2 and the parameters in Table 1. Capital letters in a through e refer to the fluxes shown in Figure 2.

levels found in plants cultured on Cho-containing medium (Nuccio et al., 1998). The position of the P-Cho signal indicates that it is in a compartment whose pH is comparable with that of the compartment containing Glc-6-P and one of the inorganic phosphate (P_i) signals; that is, the cytoplasm at a pH close to 7.5. (This compartmental assignment was made by comparison to literature values [Bligny et al., 1989, 1990] and to spectra of P-Cho solutions of defined pH; not shown).

This observation of P-Cho accumulation in a compartment of near-neutral pH was made in leaf tissue from plants grown under greenhouse conditions and in axenic culture with or without Cho (not shown). If there were a significant P-Cho storage pool in the vacuole its signal would be expected to have appeared slightly to the right of the vacuolar P_i signal in Figure 5A. No evidence of such a signal was seen in these or other spectra, even when the vacuolar P_i peak was smaller and/or narrower than in Figure 5A (not shown).

To further eliminate the possibility that a small vacuolar P-Cho signal might have been obscured by overlap with vacuolar P_i , we rapidly alkalinized both the vacuole and cytoplasm by perfusion with ammonia-containing solution. Under these conditions all compartments would be expected to come to the same elevated pH and signals from any vacuolar P-Cho would be shifted to join the cytoplasmic P-Cho peak. There was no change in the amplitude of the P-Cho peak under such conditions (not shown) supporting the view that there was no additional P-Cho pool in this tissue that was not seen at physiological pH. Besides confirming a cytoplasmic location for P-Cho, other *in vivo* NMR observations were in agreement with the model. (a) No measurable (less than $50 \mu\text{M}$) accumulation of cytidyldiphosphate choline (CDP-Cho) or glycerophosphorylcholine oc-

curred even when high levels of P-Cho accumulated. (b) Leaf tissue from Cho-grown plants, which contain high levels of Cho (Nuccio et al., 1998), gave a P-Cho signal corresponding to a cytoplasmic concentration in the low millimolar range. Perfusion of this tissue with $100 \mu\text{M}$ Cho resulted in a further accumulation of P-Cho at similar rates to that of tissue from plants grown without exogenous Cho. This supports the view that much of the accumulated Cho is in a non-metabolic pool, since exogenous Cho resulted in further cytoplasmic P-Cho accumulation whereas the high level of endogenous Cho was not being converted to P-Cho.

Metabolic Engineering Applications

Thus far we have used the model to describe the fluxes occurring in CMO^+ tobacco and to deduce the kinetic properties of the reactions and transport steps of the network. We now illustrate the usefulness of the model in generating testable hypotheses concerning metabolic engineering strategies to enhance GlyBet production without seriously reducing the net flux to Ptd-Cho, which is essential to growth. Our target flux to GlyBet was $350 \text{ pmol min}^{-1} \text{ g}^{-1}$ fresh weight because this is the rate required to sustain a GlyBet pool of $5 \mu\text{mol g}^{-1}$ fresh weight, assuming a tissue growth rate of $10\% \text{ d}^{-1}$. A tissue GlyBet content of $5 \mu\text{mol g}^{-1}$ fresh weight is within the range characteristic of GlyBet-accumulating plants and would be expected to confer significant protective effects (Sakamoto et al., 1998). To introduce and illustrate the results of our simulations, Figure 6 shows the impact of some single-parameter changes: engineering a higher CMO level, increasing the rate of Cho uptake into the chloroplast, and lowering Cho kinase expression.

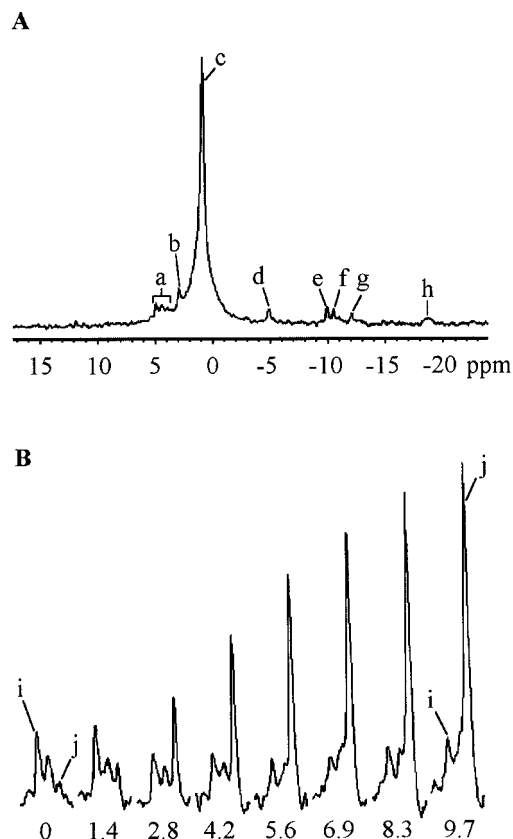


Figure 5. In vivo ^{31}P NMR analyses of CMO^+ tobacco leaf tissue. The leaf tissue was from plants that had been cultured axenically for 4 weeks on medium without Cho. A, In vivo ^{31}P NMR spectrum (acquired over 1.4 h) showing signals from: a, phosphomonoesters; b, cytoplasmic P_i ; c, vacuolar phosphate; d, the γ -phosphate of NTP; e, the α -phosphate of NTP; f, UDP-Glc with contribution from NAD(P)(H); g, UDP-Glc; and h, the β -phosphate of NTP. B, Subspectra of the phosphomonoester signals during a time-course of perfusion with $100 \mu\text{M}$ Cho. A series of eight successive spectra of the same sample as in A were acquired for 1.3 or 1.4 h each during 11.1 h of perfusion. Numbers below spectra are the time (h) at which acquisition was started. Peak i is Glc-6-P and peak j is P-Cho; both are at positions corresponding to a pH close to 7.5. Assuming an initial P-Cho content of 70 nmol g^{-1} fresh weight (Nuccio et al., 1998), the maximum rate of P-Cho accumulation (between 1.4 and 5.6 h) was estimated as approximately $5 \text{ nmol min}^{-1} \text{ g}^{-1}$ fresh weight, which is in good agreement with the V_{max} values for flux B in Table I.

Figure 6A shows that a 35-fold increase in the V_{max} of CMO does not increase flux to GlyBet at all because control resides in the previous step in the pathway, Cho uptake into the chloroplast. Thus when the capacity for Cho uptake is enhanced (Fig. 6B) there is a near-proportional increase in flux to GlyBet. However, it should be noted that flux to GlyBet cannot be increased indefinitely in this way, for two reasons. First, the activity of CMO eventually becomes limiting. Second, without an increase in the synthesis of P-Cho via the P-base pathway (or Ptd-Cho via the Ptd-base route), only a modest Cho flux can be diverted to GlyBet without causing the net flux to

Ptd-Cho to sink below the minimum needed for growth, i.e. approximately $90 \text{ pmol min}^{-1} \text{ g}^{-1}$ fresh weight (see above). Figure 6C makes a similar point: Decreasing Cho kinase activity (which increases Cho_{cy}) causes a modest increase in GlyBet synthesis, but this effect is soon vitiated by a collapse in the net flux to Ptd-Cho. The results of further manipulations of the parameters in Figure 6, other model parameters, and their combinations led to the following hypotheses.

Major gains in GlyBet synthesis in CMO^+ tobacco plants cannot be achieved without increasing the supply of Cho available in the chloroplast. A dramatic increase in GlyBet synthesis rate is observed (from 0.8 to $78 \text{ pmol min}^{-1} \text{ g}^{-1}$ fresh weight) when the rate constant for Cho flux across the chloroplast envelope is increased 150-fold (Fig. 6B). This rate could sustain a GlyBet pool of $1.1 \mu\text{mol g}^{-1}$ fresh weight in a leaf growing at $10\% \text{ d}^{-1}$, without pushing

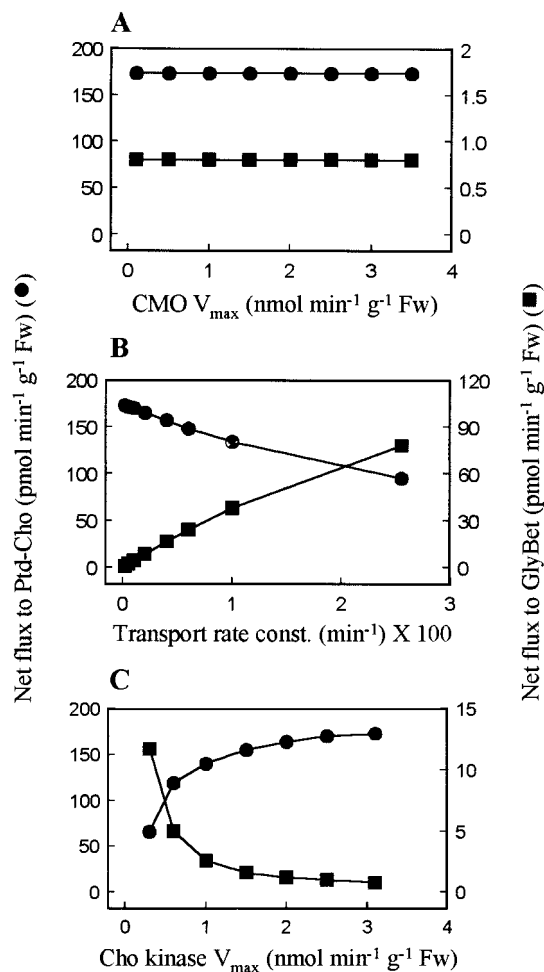


Figure 6. Simulation of the flux to GlyBet and the net flux to Ptd-Cho using the model described in Figure 2, assuming different metabolic engineering interventions. The net flux to Ptd-Cho is equal to synthesis (flux M + flux D) minus catabolism (flux E + flux H). A, Increasing the V_{max} of CMO up to 35-fold. B, Increasing the rate constant for Cho transport across the chloroplast envelope up to 150-fold. C, Decreasing the V_{max} of Cho kinase up to 11-fold.

net Ptd-Cho synthesis below the estimated threshold for normal growth of approximately $90 \text{ pmol min}^{-1} \text{ g}^{-1}$ fresh weight. It is interesting that this predicted ceiling in GlyBet level is exceeded by up to 2-fold in tobacco transgenics expressing bacterial Cho oxidase genes in the cytosol, where the chloroplast membrane is not a constraint, but these plants show significantly impaired growth (Huang et al., 2000). The results of our modeling suggest that one reason for this impairment may be the insufficient production of Ptd-Cho.

Increasing GlyBet synthesis much beyond $78 \text{ pmol min}^{-1} \text{ g}^{-1}$ fresh weight would encroach on the Ptd-Cho synthesis requirements for growth. This problem would be exacerbated were Cho kinase to be down-regulated in order to elevate cytosolic Cho levels because slowed P-Cho synthesis from Cho would further reduce the rate of Ptd-Cho synthesis (Fig. 6C). These difficulties can be overcome by increasing the flux from the P-base methylation pathway by enough to match the increased Cho demand for GlyBet synthesis. Fluxes to GlyBet in excess of $100 \text{ pmol min}^{-1} \text{ g}^{-1}$ fresh weight would also require CMO activity to be increased.

A flux to GlyBet of close to $350 \text{ pmol min}^{-1} \text{ g}^{-1}$ fresh weight (adequate to maintain a GlyBet pool of $5 \text{ } \mu\text{mol g}^{-1}$ fresh weight) can be achieved with a combination of four interventions: increasing the rate constant for Cho flux across the chloroplast envelope 3,000-fold; decreasing the V_{max} of Cho kinase 30-fold; increasing the V_{max} of CMO at least 3.5-fold; and increasing the de novo synthesis flux of P-Cho 4- to 8-fold. There is some uncertainty about this last figure as it is sensitive to assumptions about how much, if at all, the Ptd-Cho pool can expand beyond the normal range of approximately 1.3 to $2.3 \text{ } \mu\text{mol g}^{-1}$ fresh weight (McNeil et al., 2000).

These model-generated hypotheses are obviously subject to caveats. Gene expression changes might accompany and accommodate altered Cho demand in engineered plants, as occurs in yeast (Henry and Patton-Vogt, 1998). Further controls may operate at the enzyme level within the Cho metabolism network. However, because these considerations apply to steps lying upstream of Cho transport into the chloroplast and oxidation to GlyBet, they are peripheral to the central issue of diverting more Cho flux to GlyBet. They are therefore unlikely to invalidate many of the model's predictions.

CONCLUSIONS

The computer simulation model described here was designed to identify the processes in the Cho metabolism network of CMO⁺ tobacco plants that constrain GlyBet accumulation. Qualitative reasoning led Nuccio et al. (1998) to suggest that the small size of the cytosolic Cho pool, a low capacity for P-Cho synthesis, and a low rate of Ptd-Cho turnover

could all be involved. Quantitative flux modeling supported the first two of these possibilities, and suggested two others: an inadequate capacity to transport Cho into the chloroplast and excessive Cho kinase activity. The finding that large gains in GlyBet accumulation require the introduction of a high affinity, high capacity Cho transporter into the chloroplast membrane draws attention to an interesting area for basic research, for nothing is known about how Cho moves from cytosol to chloroplast.

Our results provide good examples of the "quantitative conclusions that are possible when quantification and the mathematics of quantification become part of the arsenal of investigators of metabolic interactions" (Koshland, 1998). When used in a metabolic engineering context, it is clear that modeling cannot only help decide which enzymes or transporters to target in further rounds of engineering to overcome constraints, but can also suggest by how much to change their flux capacities or affinity constants in order to attain specific engineering goals.

MATERIALS AND METHODS

Plant Material

All experiments were carried out with vegetatively propagated primary transformants of tobacco (*Nicotiana tabacum* L. cv Wisconsin 38) expressing spinach CMO (CMO⁺ tobacco; line 4, Nuccio et al., 1998). Plants for [¹⁴C]Cho labeling were grown in a light soil mix in a naturally lit greenhouse; the minimum temperature was 18°C. Irrigation was with 0.5× Hoagland nutrient solution. Half or fully expanded leaves from mature plants that had not flowered were harvested between February and May 1998. Plants for ³¹P NMR experiments were grown as above, or cultured axenically for 4 weeks on medium plus or minus 5 mM Cho (Nuccio et al., 1998).

Radiolabeling Experiments

[Methyl-¹⁴C]Cho (54 mCi mmol⁻¹) was obtained from NEN (Boston) and purified as described (Weigel et al., 1988). Discs (11 mm in diameter) were cut from the mid-blade region of a single leaf for each experiment. Eight shallow radial incisions were made on the abaxial surface of each disc. Samples were batches of three discs (approximately 50 mg fresh weight). Labeled solutions were applied (2 μL per disc) to the incisions; the discs were then incubated, abaxial surface uppermost, on moist filter paper circles in Petri dishes at $25^\circ\text{C} \pm 2^\circ\text{C}$ in fluorescent light (photosynthetic photon flux density $150 \text{ } \mu\text{E m}^{-2} \text{ s}^{-1}$).

Analysis of Labeled Metabolites

Procedures were essentially as described (Hanson and Rhodes, 1983; Nuccio et al., 1998; McNeil et al., 2000). Briefly, discs were extracted by a methanol-chloroform-water procedure after boiling in isopropanol to denature phospholipases, and organic and aqueous phases were

separated. Radioactivity in both phases was quantified by scintillation counting. The only labeled metabolite in the organic phase was shown to be Ptd-Cho by thin-layer chromatography. Water-soluble metabolites were fractionated by ion-exchange using 1-mL columns of AG-1 (OH⁻), BioRex-70 (H⁺), and AG-50 (H⁺) arranged in series; P-Cho was eluted from AG-1 with 5 mL of 2.5 N HCl, Cho from BioRex-70 with 5 mL of 1 N HCl, and GlyBet from AG-50 with 5 mL of 2.5 N HCl. The identities of the labeled metabolites in the eluates were confirmed by thin-layer chromatography. Glycerophosphorylcholine, which appears in the effluent from the three-column series, was found not to acquire appreciable label. Data were corrected for recovery by using samples spiked with [¹⁴C]P-Cho, [¹⁴C]Cho, or [¹⁴C]GlyBet.

Computer Modeling of Labeling Data

The computer model was evolved from that described by McNeil et al. (2000). Models were implemented with programs written in Microsoft Visual Basic. Key assigned parameters were the initial pool sizes, their specific activities, and the rates connecting the various pools. Most flux rates (v) were assumed to respond to substrate pool size (S) according to the Michaelis-Menten equation, i.e. $v = (V_{\max} \times S)/(K_m + S)$, where individual V_{\max} and K_m values were specified for each enzyme reaction or transport step. In time-course simulations the assigned parameters and existing substrate pool sizes were used to calculate how much material of defined specific activity was drawn from one pool to another during 0.1-min intervals. During each iteration new specific activities and pool sizes were computed, and total radioactivity in each pool plotted (superimposed on observed data) as a function of time. Model values and initial pool sizes were progressively adjusted (within limits set by experimentally determined or literature values) until a close match between observed and simulated radioactivity was obtained for the time-course, as judged graphically or by computing mean absolute deviations between observed and simulated values. Further details on our models are available at <http://www.hort.purdue.edu/cfesp/models/models.htm>.

³¹P NMR

Leaves were cut into 2- to 4-mm wide strips and vacuum infiltrated for 1 to 3 s in a 1 mM CaSO₄ solution. Approximately 2 g of tissue was packed in a 10-mm diameter NMR tube and perfused with aerated 1 mM CaSO₄ (flow rate 2–5 mL min⁻¹) at approximately 18°C. For incubation with Cho, 100 μM Cho chloride was added to the perfusion medium. Alkalinization was induced by perfusing with 1 mM CaSO₄ containing 30 mM NH₄Cl at pH 9.0. ³¹P NMR spectra were acquired on a UnityPlus 600 MHz instrument (Varian Inc., Palo Alto, CA) using a 10 mm Broadband probe. Acquisition conditions were: 90° pulses, a recycle time of 1 s, and no lock or decoupling; acquisition times for time-courses were 1 to 3 h per spectrum except for alkalinization experiments where they were 7 min. Data were

processed with minimal exponential multiplication (line broadening of 10–30 Hz for in vivo spectra) and Fourier transformation using spectrometer software. Peak assignments and referencing were made by reference to literature values and to spectra of external solutions of P_i, P-Cho, and CDP-Cho buffered at cytoplasmic (7.5) or vacuolar (approximately 5) pH (Chang and Roberts, 1992; Y. Shachar-Hill and D. Brauer, unpublished data). Chemical shift values in spectra are given in reference to 85% phosphoric acid at 0 ppm.

MODEL DEVELOPMENT

We began model development using data for metabolism of [¹⁴C]Cho by half-expanded leaves of CMO⁺ plants because the endogenous pool sizes and fluxes of Cho metabolites are well documented for young tobacco leaves (Nuccio et al., 1998; McNeil et al., 2000). The model we built is shown in Figure 2; its main features and their rationales are as follows.

Metabolite Pools

The initial sizes of the endogenous pools of Cho, betaine aldehyde (BetAld), GlyBet, P-Cho, and Ptd-Cho were based on measured values (Nuccio et al., 1998; McNeil et al., 2000). The model posits a small metabolically active pool of Cho in the cytosol (Cho_{cy}, 2 nmol g⁻¹ fresh weight), a large vacuolar storage pool (Cho_{vac}, 75 nmol g⁻¹ fresh weight; Hanson and Rhodes, 1983; McNeil et al., 2000), and a small chloroplastic pool (Cho_{chl}, 0.2 nmol g⁻¹ fresh weight) serving as substrate for GlyBet production. These three pools sum to the measured total free Cho value in CMO⁺ tobacco (Nuccio et al., 1998). There are single pools of BetAld, GlyBet, P-Cho, and Ptd-Cho, the Ptd-Cho pool (1,800 nmol g⁻¹ fresh weight) being far larger than any other in the network. Because BetAld was not detectable, its pool size was set to the detection limit of approximately 0.2 nmol g⁻¹ fresh weight (Rhodes et al., 1987). There is a single, cytosolic P-Cho pool because the modeling of radiotracer data on Cho synthesis in tobacco suggested this feature (McNeil et al., 2000). The GlyBet pool is assumed not to turn over because tobacco was found not to catabolize GlyBet (Nuccio et al., 1998).

Transport Fluxes

Uptake of Cho from the apoplast has the characteristics of passive diffusion at Cho concentrations > 100 μM (Bligny et al., 1989). Assuming the apoplast to be approximately 5% of leaf volume (Winter et al., 1994), the initial apoplastic [¹⁴C]Cho levels in this study were approximately 3 mM; Cho uptake (flux A) is accordingly modeled as a passive flux. The kinetics of Cho movement between cytosol and vacuole are modeled as a “pump-leak” system, with active import into the vacuole (flux G) and passive efflux to the cytosol (flux F). Active uptake via a saturable carrier is invoked since Cho_{vac} is much larger than Cho_{cy}, and the membrane potential across the tonoplast does not

favor Cho influx (Rea and Poole, 1993); passive leakage is the simplest mechanism to explain efflux from the vacuole. Cho uptake into the chloroplast (flux I) is also modeled as a passive process because no literature suggests a more complex mechanism, and our data do not require one. Note that this process could correspond to diffusion or to a saturable, carrier-mediated process whose K_m is higher than the Cho_{cy} values that were reached in our experiments. Passive fluxes are proportional to the sizes of their substrate pools (Fick's first law), and are described by first-order rate constants (Table I); uptake into the vacuole is characterized by a V_{max} and a K_m (see below). Cho efflux from the chloroplast and from the cytosol to the apoplast are assumed to be negligible due to the low Cho concentrations in these compartments. Nor was GlyBet efflux from the chloroplast considered, since the model cannot address the location of an inert end product.

Metabolic Fluxes

The model provides for P-Cho and Ptd-Cho synthesis from unlabeled endogenous precursors (fluxes L and M). While these fluxes add no ^{14}C to the system they contribute to P-Cho and Ptd-Cho turnover and, in the absence of supplied Cho, they are the sole sources of new Cho moieties. These fluxes are assigned constant rates (0.12 and 0.02 $nmol\ min^{-1}\ g^{-1}$ fresh weight for P-Cho and Ptd-Cho synthesis, respectively) that lie within the ranges obtained from the modeling of ^{33}P -base and [^{14}C]formate tracer kinetics (McNeil et al., 2000).

Other metabolic fluxes were assumed to be mediated by Michaelian enzymes and hence to show saturable responses to substrate pool size. These fluxes are therefore assigned a V_{max} ($nmol\ min^{-1}\ g^{-1}$ fresh weight) and an apparent K_m ($nmol\ g^{-1}$ fresh weight), as summarized in Table I. V_{max} and K_m values were interconverted between the fresh weight-based units required in the model and the customary units of $nmol\ min^{-1}\ mg^{-1}$ protein and μM by assuming a leaf protein content of 10 $mg\ g^{-1}$ fresh weight, a chlorophyll (Chl) content of 1 $mg\ g^{-1}$ fresh weight, and the following subcellular compartment volumes (Winter et al., 1994): cytosol, 24 $\mu L\ mg^{-1}$ Chl; chloroplast stroma, 66 $\mu L\ mg^{-1}$ Chl; and vacuole, 546 $\mu L\ mg^{-1}$ Chl.

Ptd-Cho synthesis from P-Cho proceeds in two steps via the intermediate CDP-Cho. However, as the CTP:P-Cho cytidyltransferase catalyzing the first step appears to exert most of the control over flux (Price-Jones and Harwood, 1986; Kinney et al., 1987), and since the level of CDP-Cho in tobacco was below the detection limit, for simplicity we treated the P-Cho \rightarrow CDP-Cho \rightarrow Ptd-Cho reactions as a single process (flux D) that largely reflects the properties of the cytidyltransferase. The model postulates that Ptd-Cho is catabolized to Cho_{cy} via phospholipase D (flux H), or to P-Cho (e.g. via phospholipase C; flux E), and that P-Cho is converted to Cho_{cy} by phosphatase activity and/or the reverse reaction of Cho kinase (flux C; McNeil et al., 2000).

Enzyme data were used to assign V_{max} and K_m values to the $Cho_{chl} \rightarrow$ BetAld \rightarrow GlyBet steps (fluxes J and K). CMO

activities in unsalinized and salinized CMO⁺ leaves were estimated to be 0.1 and 0.3 $nmol\ min^{-1}\ g^{-1}$ fresh weight, respectively (Nuccio et al., 1998; S. McNeil, unpublished data). BADH activity in tobacco leaves is 3 to 10 $nmol\ min^{-1}\ g^{-1}$ fresh weight (Rathinasabapathi et al., 1994; Trossat et al., 1997), and approximately 20% of BADH was shown to be chloroplastic (S. McNeil, unpublished data). We therefore assigned a V_{max} value of 1 $nmol\ min^{-1}\ g^{-1}$ fresh weight to chloroplastic BADH. The K_m value for spinach CMO is 100 μM (Brouquisse et al., 1989); that for BADH was taken to be 50 μM , the value for spinach BADH expressed in tobacco chloroplasts (Trossat et al., 1997).

Other Models Tested

Several plausible variations of the model were tested, alone and in combination, using the experimental data for immature leaves. These included models in which (a) Cho import into the chloroplast is mediated by a saturable transporter, (b) the expansion of the P-Cho pool caused by the rapid influx of [^{14}C]Cho transiently inhibits de novo P-Cho and Ptd-Cho synthesis (Mudd and Datko, 1989), (c) P-Cho inhibits phospholipase C (Berka and Vasil, 1982), and (d) Cho kinase has a 20-fold lower K_m for Cho_{cy} than shown in Table I. None of these variations substantially improved the goodness-of-fit between simulated and observed values.

ACKNOWLEDGMENT

We thank Dr. Steven J. Blackband for assistance with NMR analyses at the University of Florida.

Received February 29, 2000; accepted May 19, 2000.

LITERATURE CITED

- Bailey JE (1998) Mathematical modeling and analysis in biochemical engineering: past accomplishments and future opportunities. *Biotechnol Prog* **14**: 3–20
- Berka RM, Vasil ML (1982) Phospholipase C (heat-labile hemolysin) of *Pseudomonas aeruginosa*: purification and preliminary characterization. *J Bacteriol* **152**: 239–245
- Bligny R, Foray M-F, Roby C, Douce R (1989) Transport and phosphorylation of choline in higher plant cells: phosphorus-31 nuclear magnetic resonance studies. *J Biol Chem* **264**: 4888–4895
- Bligny R, Foray M-F, Roby C, Douce R (1990) ^{31}P NMR studies of spinach leaves and their chloroplasts. *J Biol Chem* **265**: 1319–1326
- Brouquisse R, Weigel P, Rhodes D, Yocum CF, Hanson AD (1989) Evidence for a ferredoxin-dependent choline monooxygenase from spinach chloroplast stroma. *Plant Physiol* **90**: 322–329
- Chang KJ, Roberts JKM (1992) Observations of cytoplasmic and vacuolar malate in maize root tips by ^{13}C NMR spectroscopy. *Plant Physiol* **89**: 197–203
- Fell DA (1997) *Understanding the Control of Metabolism*. Portland Press, London

- Gawer M, Guern N, Chervin D, Mazliak P** (1991) Choline kinase activities in choline-sensitive and choline-resistant tobacco cells or calluses grown on high choline concentrations: effects on phosphatidylcholine synthesis. *Plant Sci* **75**: 167–176
- Guynn RW** (1976) Equilibrium constants under physiological conditions for the reactions of choline kinase and the hydrolysis of phosphorylcholine to choline and inorganic phosphate. *J Biol Chem* **251**: 7162–7167
- Hanson AD, Rhodes D** (1983) ^{14}C tracer evidence for synthesis of choline and betaine via phosphoryl base intermediates in salinized sugar beet leaves. *Plant Physiol* **71**: 692–700
- Henry SA, Patton-Vogt JL** (1998) Genetic regulation of phospholipid metabolism: yeast as a model eukaryote. *Prog Nucleic Acid Res Mol Biol* **61**: 133–179
- Huang J, Hirji R, Adam L, Rozwadowski K, Hammerlindl J, Keller W, Selvaraj G** (2000) Genetic engineering of glycinebetaine production toward enhancing stress tolerance in plants: metabolic limitations. *Plant Physiol* **122**: 747–756
- Kinney AJ, Clarkson DT, Loughman BC** (1987) The regulation of phosphatidylcholine biosynthesis in rye (*Secale cereale*) roots: stimulation of the nucleotide pathway by low temperature. *Biochem J* **242**: 755–759
- Koshland DE Jr** (1998) The era of pathway quantification. *Science* **280**: 852–853
- McNeil SD, Nuccio ML, Hanson AD** (1999) Betaines and related osmoprotectants: targets for metabolic engineering of stress resistance. *Plant Physiol* **120**: 945–949
- McNeil SD, Nuccio ML, Rhodes D, Shachar-Hill Y, Hanson AD** (2000) Radiotracer and computer modeling evidence that phosphobase methylation is the main route of choline synthesis in tobacco. *Plant Physiol* **123**: 371–380
- Mongrand S, Bessoule JJ, Cassagne C** (1997) A re-examination of the phosphatidylcholine-galactolipid relationship during plant lipid biosynthesis. *Biochem J* **327**: 853–858
- Mudd SH, Datko AH** (1989) Synthesis of methylated ethanolanamine moieties: regulation by choline in *Lemna*. *Plant Physiol* **90**: 296–305
- Nuccio ML, Rhodes D, McNeil SD, Hanson AD** (1999) Metabolic engineering of plants for osmotic stress resistance. *Curr Opin Plant Biol* **2**: 128–134
- Nuccio ML, Russell BL, Nolte KD, Rathinasabapathi B, Gage DA, Hanson AD** (1998) The endogenous choline supply limits glycine betaine synthesis in transgenic tobacco expressing choline monooxygenase. *Plant J* **16**: 101–110
- Price-Jones MJ, Harwood JL** (1986) The control of CTP: choline-phosphate cytidylyltransferase activity in pea (*Pisum sativum* L.). *Biochem J* **240**: 837–842
- Rathinasabapathi B, McCue KF, Gage DA, Hanson AD** (1994) Metabolic engineering of glycine betaine synthesis: plant betaine aldehyde dehydrogenases lacking typical transit peptides are targeted to tobacco chloroplasts where they confer betaine aldehyde resistance. *Planta* **193**: 155–162
- Rea PA, Poole RJ** (1993) Vacuolar H^+ -translocating pyrophosphatase. *Annu Rev Plant Physiol Plant Mol Biol* **44**: 157–180
- Rhodes D, Rich PJ, Myers AC, Reuter CC, Jamieson GC** (1987) Determination of betaines by fast atom bombardment mass spectrometry: identification of glycinebetaine deficient genotypes of *Zea mays*. *Plant Physiol* **84**: 781–788
- Sakamoto A, Alia, Murata N** (1998) Metabolic engineering of rice leading to biosynthesis of glycine betaine and tolerance to salt and cold. *Plant Mol Biol* **38**: 1011–1019
- Setty PN, Krishnan PS** (1972) Choline kinase in *Cuscuta reflexa*. *Biochem J* **126**: 313–324
- Stephanopoulos G** (1999) Metabolic fluxes and metabolic engineering. *Metab Eng* **1**: 1–11
- Stephanopoulos G, Vallino JJ** (1991) Network rigidity and metabolic engineering in metabolite overproduction. *Science* **252**: 1675–1681
- Tanaka K, Tolbert NE, Gohlke AF** (1966) Choline kinase and phosphorylcholine phosphatase in plants. *Plant Physiol* **41**: 307–312
- Trossat C, Rathinasabapathi B, Hanson AD** (1997) Transgenically-expressed betaine aldehyde dehydrogenase efficiently catalyzes oxidation of dimethylsulfoniopropionaldehyde and ω -aminoaldehydes. *Plant Physiol* **113**: 1457–1461
- Wang XM, Moore TS Jr** (1989) Partial purification and characterization of CTP:cholinephosphate cytidylyltransferase from castor bean endosperm. *Arch Biochem Biophys* **274**: 338–347
- Weigel P, Lerma C, Hanson AD** (1988) Choline oxidation by intact spinach chloroplasts. *Plant Physiol* **86**: 54–60
- Winter H, Robinson DG, Heldt HW** (1994) Subcellular volumes and metabolite concentrations in spinach leaves. *Planta* **193**: 530–535